

Robust Adaptive Quantum Phase Estimation

Shibdas Roy^{1,2,*}, Ian R. Petersen¹ and Elanor H. Huntington^{2,3}

¹School of Engineering and Information Technology, University of New South Wales, Australian Defence Force Academy, Canberra

²Australian Research Council Centre of Excellence for Quantum Computation and Communication Technology, Australia

³College of Engineering and Computer Science, Australian National University, Canberra

E-mail: *roy_shibdas@yahoo.co.in

Abstract. Quantum parameter estimation is central to many fields such as quantum computation, communications and metrology. Optimal estimation theory has been instrumental in achieving the best accuracy in quantum parameter estimation, which is possible when we have very precise knowledge of and control over the model. However, uncertainties in key parameters underlying the system are unavoidable and may impact the quality of the estimate. We show here how quantum optical phase estimation of a squeezed state of light exhibits improvement when using a robust fixed-interval smoother designed with uncertainties explicitly introduced in parameters underlying the phase noise.

Keywords: quantum phase estimation, robust estimator, optimal estimator, smoothing, squeezed state.

1. Introduction

Quantum parameter estimation [1] is the problem of estimating a classical variable of a quantum system. It plays a key role in quantum computation [2], quantum communications [3, 4], quantum key distribution [5], metrology [6] and gravitational wave interferometry [7], etc. A common and technologically relevant example is estimating an optical phase in a quantum system. Optimal estimation theory has earlier been considered in devising and improving quantum parameter estimation techniques. Systematic approaches to optimal estimation yield estimates with the lowest mean-square estimation error. This has helped achieve better estimation accuracies than otherwise obtained previously [8, 9].

Nonetheless, the optimality of the estimation process relies on precise knowledge of the system model. However, this is usually unrealistic due to inevitable modelling errors. In many cases, it is impossible to precisely measure and determine values of relevant model parameters in an experiment. This is detrimental in problems of quantum estimation because any uncertainty in our knowledge of the parameters in the system model may result in considerable degradation in the estimation accuracy. It is, therefore, desired to make the estimation process robust to uncertainties in the underlying model parameters [10, 11].

It is important in many practical engineering problems to ensure that the critical measures of the system performance do not deviate beyond certain thresholds. Such thresholds mark the point beyond which the system has a high risk of breaking down or becoming unusable. In quantum estimation problems, the performance is typically determined by the error in the estimation process in the presence of uncertainty in the system. A robust estimator would guarantee that the worst-case estimation error is lower than a critical level of accuracy. For example, in gravitational wave detection, large estimation errors may mask a gravitational-wave event or imitate an event. Such a false event may be avoided using a robust estimator, which has a guaranteed worst-case precision.

In this paper, we aim to design a robust estimator for quantum phase estimation that provides guaranteed worst-case performance. Robust quantum parameter estimation was previously considered in Ref. [12] for magnetometry. That paper employed heuristic feedback mechanism to achieve robustness. By contrast, we consider a more systematic approach to robust estimation in a state-space setting with explicitly modelled uncertainty. Among other related works, Ref. [13] proposed a robust quantum observer for uncertain linear quantum systems and Ref. [14] considered robustness in the context of coherent feedback. However, for linear quantum systems, much of the rich classical estimation theory may be applied. To our knowledge, the potential application of classical robust estimation theory has not yet been explored in improving quantum estimation techniques.

Quantum phase estimation has been area of active research recently [15–22]. Adaptive quantum phase estimation of the continuously varying phase of a coherent

state of light using smoothing was demonstrated in Ref. [8]. Fixed-interval smoothing uses both past and future measurements in a fixed time-interval to yield a more accurate estimate than obtained using only past measurements [23–30]. Using a robust fixed-interval smoother [31], the estimation process for the adaptive experiment can be improved in the presence of uncertainty in the underlying phase noise subject to an Ornstein-Uhlenbeck (OU) noise [32]. While a coherent state has the same uncertainty in both (amplitude and phase) quadratures, a squeezed state has reduced fluctuations in one of the two quadratures at the expense of increased fluctuations in the other. Using a squeezed state of light provides quantum enhancement in adaptive phase tracking [9]. Here, we illustrate the guaranteed worst-case performance of the robust estimator for such a squeezed state [33].

The robust fixed-interval smoothing scheme can as well be applied to estimate a phase, modelled as a resonant noise process with uncertainty in its parameters [34]. A related robust filtering problem for coherent state was considered by the authors for OU process in Ref. [35] and for resonant process in Ref. [36]. Here, we build on the results in the conference paper [34] to provide interesting insights about the guaranteed worst-case performance of the robust estimator. Moreover, we show that the performance improvement of the robust estimator relative to the optimal estimator grows as the noise process becomes more resonant. We also show here that the worst-case performance of our robust estimator relative to the optimal estimator is better for realistic lossy squeezed beams than that for ideal pure squeezed beams at the optimal degrees of squeezing. In addition, we illustrate that our robust estimator exhibits an optimal photon number for which its relative performance is the best with respect to the optimal estimator.

2. Optimal Estimator

The optimal estimator in Ref. [9] involves an offline optimal smoother, in addition to a Kalman filter in the feedback loop. The feedback Kalman filter is a causal filter. However, the smoother is acausal, since it is, in principle, a combination of a forward-time Kalman filter and a backward-time Kalman filter, the estimates of which are combined to yield the optimal smoothed estimate [37]. While the forward Kalman filter is essentially the feedback filter itself and uses only past measurements, the backward filter yields its estimate based on future measurements with respect to the time of the desired smoothed estimate within the chosen fixed time-interval. A smoother, therefore, cannot be used to produce real-time estimates, and is usually used for offline data processing or with a delay with respect to the estimation time to yield more accurate estimates than obtained using the feedback Kalman filter alone [8, 9].

2.1. System Model

We need to define our system in terms of the process and measurement models in a state-space setting.

The process model is the OU noise process that modulates the phase $\phi(t)$, to be estimated, of the continuous optical phase-squeezed beam [9]:

$$\dot{\phi}(t) = -\lambda\phi(t) + \sqrt{\kappa}v(t), \quad (1)$$

where $\lambda^{-1} > 0$ is the correlation time of $\phi(t)$, $\kappa > 0$ is the phase variation magnitude and $v(t)$ is a zero-mean white Gaussian noise with unity amplitude.

The phase-modulated beam is measured by homodyne detection using a local oscillator, the phase of which is adapted with the filtered estimate $\hat{\phi}_f(t)$ using feedback, thereby yielding a normalized homodyne output photocurrent [9]:

$$I(t)dt \simeq 2|\alpha|[\phi(t) - \hat{\phi}_f(t)]dt + \sqrt{\overline{R}_{sq}}dW(t), \quad (2)$$

$$\overline{R}_{sq} = \sigma_f^2 e^{2r_p} + (1 - \sigma_f^2)e^{-2r_m}, \quad (3)$$

where $|\alpha|$ is the amplitude of the input phase-squeezed beam, and $W(t)$ is a Wiener process arising from squeezed vacuum fluctuations. The parameter \overline{R}_{sq} is determined by the degree of squeezing ($r_m \geq 0$) and anti-squeezing ($r_p \geq r_m$) and by σ_f^2 (see later). We use the measurement appropriately scaled as our measurement model [33]:

$$\theta(t) := \frac{2|\alpha|}{\sqrt{\overline{R}_{sq}}}\phi(t) + w(t), \quad (4)$$

where $w := \frac{dW}{dt}$ is also a zero-mean white Gaussian noise with unity amplitude.

Here, $E[v(t)v(\tau)] = N\delta(t - \tau)$, $E[w(t)w(\tau)] = S\delta(t - \tau)$, $E[v(t)w(\tau)] = 0$, where $E[\cdot]$ denotes the expectation value and $\delta(\cdot)$ is the delta function. Since v and w are of unity amplitude, both N and S are unity.

2.2. Forward Filter

The steady-state Riccati equation to be solved for the forward Kalman filter is [37]:

$$-2\lambda P_f - \frac{4|\alpha|^2}{\overline{R}_{sq}}P_f^2 + \kappa = 0, \quad (5)$$

where $P_f = \sigma_f^2$ is the forward filter error-covariance. The stabilising solution of the above equation is:

$$P_f = \frac{\overline{R}_{sq}}{4|\alpha|^2} \left(-\lambda + \sqrt{\lambda^2 + \frac{4\kappa|\alpha|^2}{\overline{R}_{sq}}} \right). \quad (6)$$

The forward filter equation is [37]:

$$\dot{\hat{\phi}}_f = -(\lambda + K_f)\hat{\phi}_f + \frac{2|\alpha|K_f}{\sqrt{\overline{R}_{sq}}}\phi + K_f w, \quad (7)$$

where $K_f = \frac{\sqrt{\overline{R}_{sq}}}{2|\alpha|} \left(-\lambda + \sqrt{\lambda^2 + \frac{4\kappa|\alpha|^2}{\overline{R}_{sq}}} \right)$ is the forward Kalman gain.

2.3. Backward Filter

The steady-state Riccati equation to be solved for the backward Kalman filter is [37]:

$$2\lambda P_b - \frac{4|\alpha|^2}{\bar{R}_{sq}} P_b^2 + \kappa = 0, \quad (8)$$

where $P_b = \sigma_b^2$ is the backward filter error-covariance. The stabilising solution of the above equation is:

$$P_b = \frac{\bar{R}_{sq}}{4|\alpha|^2} \left(\lambda + \sqrt{\lambda^2 + \frac{4\kappa|\alpha|^2}{\bar{R}_{sq}}} \right). \quad (9)$$

The backward filter equation is [37]:

$$\dot{\hat{\phi}}_b = (\lambda - K_b)\hat{\phi}_b + \frac{2|\alpha|K_b}{\sqrt{\bar{R}_{sq}}}\phi + K_bw, \quad (10)$$

where $K_b = \frac{\sqrt{\bar{R}_{sq}}}{2|\alpha|} \left(\lambda + \sqrt{\lambda^2 + \frac{4\kappa|\alpha|^2}{\bar{R}_{sq}}} \right)$ is the backward Kalman gain.

2.4. Smoother Error

The smoother error, $P_s = \sigma^2$, is given by [37]:

$$P_s = (P_f^{-1} + P_b^{-1})^{-1}, \quad (11)$$

since the forward and backward estimates are independent.

3. Robust Estimator

Here, we build a robust fixed-interval smoother, corresponding to the optimal smoother above, using the technique from Ref. [31].

3.1. Uncertain Model

The uncertainty is introduced in the parameter λ as follows: $\lambda \rightarrow \lambda - \mu\Delta\lambda$, where Δ is an uncertain parameter satisfying $|\Delta| \leq 1$, and $0 \leq \mu < 1$ determines the level of uncertainty in the model. From Eq. (2.5) in Ref. [31], our uncertain process model is:

$$\dot{\phi} = -\lambda\phi + B_1\Delta K\phi + B_1v, \quad (12)$$

where $B_1 = \sqrt{\kappa}$ and $K = \mu\lambda/\sqrt{\kappa}$. The measurement model remains the same, i.e. (4). The uncertainty output from Eq. (2.1) in Ref. [31] is: $z = (\mu\lambda/\sqrt{\kappa})\phi$.

The uncertain system should satisfy an integral quadratic constraint of the form Eq. (2.4) in Ref. [31]:

$$\int_0^T (\tilde{w}^2 + \tilde{v}^2)dt \leq 1 + \int_0^T \|z\|^2 dt, \quad (13)$$

where $\tilde{w} = \Delta K\phi + v$ and $\tilde{v} = w$ are the uncertainty inputs. Here, $X_0 = 0$, since no *a-priori* information exists about the initial condition of the state. Also, $d = 1$, since the white noise processes v and w are of unity amplitude. Thus, we would have $Q = R = 1$ in our case.

3.2. Forward Filter

The steady-state forward Riccati equation, as obtained from Eq. (5.1) in Ref. [31], is:

$$-2\lambda X + \kappa X^2 + \frac{\mu^2 \lambda^2}{\kappa} - \frac{4|\alpha|^2}{\overline{R}_{sq}} = 0. \quad (14)$$

The stabilising solution of the above equation for X is:

$$X = \frac{\lambda + \sqrt{\lambda^2 - \mu^2 \lambda^2 + \frac{4|\alpha|^2 \kappa}{\overline{R}_{sq}}}}{\kappa}. \quad (15)$$

Next, Eq. (5.3) in Ref. [31] for our case yields:

$$\dot{\eta} = - \left(\sqrt{\lambda^2 - \mu^2 \lambda^2 + \frac{4|\alpha|^2 \kappa}{\overline{R}_{sq}}} \right) \eta + \frac{4|\alpha|^2}{\overline{R}_{sq}} \phi + \frac{2|\alpha|}{\sqrt{\overline{R}_{sq}}} w. \quad (16)$$

The forward filter is, then, simply the centre of the ellipse of Eq. (3.3) in Ref. [31]: $\hat{\phi}_f = \eta/X$.

Thus, the forward robust filter equation is

$$\dot{\hat{\phi}}_f = -L\hat{\phi}_f + \frac{4|\alpha|^2 \kappa}{\overline{R}_{sq}(\lambda + L)} \phi + \frac{2|\alpha| \kappa}{\sqrt{\overline{R}_{sq}}(\lambda + L)} w, \quad (17)$$

where $L = \sqrt{\lambda^2 - \mu^2 \lambda^2 + \frac{4|\alpha|^2 \kappa}{\overline{R}_{sq}}}$.

For $\mu = 0$, (17) reduces to (7), i.e. the robust forward filter is simply the forward Kalman filter for zero uncertainty level.

3.3. Backward Filter

The steady-state backward Riccati equation, as obtained from Eq. (5.2) in Ref. [31], is:

$$-2\lambda Y - \kappa Y^2 - \frac{\mu^2 \lambda^2}{\kappa} + \frac{4|\alpha|^2}{\overline{R}_{sq}} = 0. \quad (18)$$

The stabilising solution of the above equation for Y is:

$$Y = \frac{-\lambda + \sqrt{\lambda^2 - \mu^2 \lambda^2 + \frac{4|\alpha|^2 \kappa}{\overline{R}_{sq}}}}{\kappa}. \quad (19)$$

Next, Eq. (5.4) in Ref. [31] for reverse-time yields:

$$\dot{\xi} = - \left(\sqrt{\lambda^2 - \mu^2 \lambda^2 + \frac{4|\alpha|^2 \kappa}{\overline{R}_{sq}}} \right) \xi + \frac{4|\alpha|^2}{\overline{R}_{sq}} \phi + \frac{2|\alpha|}{\sqrt{\overline{R}_{sq}}} w. \quad (20)$$

The backward filter is, then, simply: $\hat{\phi}_b = \xi/Y$.

Thus, the backward robust filter equation is

$$\dot{\hat{\phi}}_b = -L\hat{\phi}_b + \frac{4|\alpha|^2 \kappa}{\overline{R}_{sq}(-\lambda + L)} \phi + \frac{2|\alpha| \kappa}{\sqrt{\overline{R}_{sq}}(-\lambda + L)} w, \quad (21)$$

where again $L = \sqrt{\lambda^2 - \mu^2 \lambda^2 + \frac{4|\alpha|^2 \kappa}{\overline{R}_{sq}}}$.

For $\mu = 0$, (21) reduces to (10), i.e. the robust backward filter is the same as the backward Kalman filter for zero uncertainty level.

3.4. Robust Smoother

The robust smoother would be the centre of the ellipse of Eq. (5.5) in Ref. [31]:

$$\hat{\phi} = \frac{\eta + \xi}{X + Y}. \quad (22)$$

4. Comparison of Estimators

We shall now compare the mean-square estimation errors of the optimal and robust estimators for the uncertain system.

4.1. Error Analysis

Given the forward and backward filter dynamics for the uncertain system, the mean-square errors for $|\Delta| \leq 1$ are computed using the following method employing a Lyapunov equation. Here, we shall illustrate the method for the optimal estimator only. The errors for the robust estimator may be calculated similarly.

4.1.1. Forward Filter The uncertain system, given by

$$\dot{\phi} = -\lambda\phi + \mu\Delta\lambda\phi + \sqrt{\kappa}v, \quad (23)$$

augmented with the forward-time Kalman filter (7) may be represented by the state-space model:

$$\dot{\bar{\mathbf{x}}} = \bar{\mathbf{A}}\bar{\mathbf{x}} + \bar{\mathbf{B}}\bar{\mathbf{w}}, \quad (24)$$

where $\bar{\mathbf{x}} = \begin{bmatrix} \phi \\ \hat{\phi}_f \end{bmatrix}$, $\bar{\mathbf{w}} = \begin{bmatrix} v \\ w \end{bmatrix}$.

Thus, we have

$$\bar{\mathbf{A}} = \begin{bmatrix} -\lambda + \mu\Delta\lambda & 0 \\ \frac{2|\alpha|K_f}{\sqrt{R_{sq}}} & -(\lambda + K_f) \end{bmatrix}, \quad \bar{\mathbf{B}} = \begin{bmatrix} \sqrt{\kappa} & 0 \\ 0 & K_f \end{bmatrix}.$$

The steady-state state covariance matrix \mathbf{P}_S is obtained by solving the Lyapunov equation:

$$\bar{\mathbf{A}}\mathbf{P}_S + \mathbf{P}_S\bar{\mathbf{A}}^T + \bar{\mathbf{B}}\bar{\mathbf{B}}^T = 0, \quad (25)$$

where \mathbf{P}_S is the symmetric matrix

$$\mathbf{P}_S = E[\bar{\mathbf{x}}\bar{\mathbf{x}}^T] = \begin{bmatrix} \Sigma & M_f \\ M_f^T & N_f \end{bmatrix}. \quad (26)$$

The estimation error can be written as:

$$e_1 = \phi - \hat{\phi}_f = [1 \ -1]\bar{\mathbf{x}}, \quad (27)$$

which is mean zero since all of the quantities determining e_1 are mean zero. The error covariance is then given as:

$$\sigma_f^2 = E[e_1 e_1^T] = \Sigma - M_f - M_f^T + N_f. \quad (28)$$

4.1.2. Backward Filter When our uncertain model (23), (4), which is driven by Gaussian white noise, has reached steady state, the output process will be a stationary Gaussian random process, which is described purely by its auto-correlation function. If we consider this output process in reverse time, this will also be a stationary random process with the same auto-correlation function. This follows from the definition of the auto-correlation function. Hence, the statistics of the reversed time output process are the same as the statistics of the forward time output process. Thus, the reversed time output process can be regarded as being generated by the same (and not time reversed) process (23) that generated the forward time process [32].

The augmented system (24) for the backward Kalman filter (10) will then have

$$\bar{\mathbf{x}} = \begin{bmatrix} \phi \\ \hat{\phi}_b \end{bmatrix}, \quad \bar{\mathbf{A}} = \begin{bmatrix} -\lambda + \mu\Delta\lambda & 0 \\ \frac{2|\alpha|K_b}{\sqrt{\bar{R}_{sq}}} & (\lambda - K_b) \end{bmatrix}, \quad \bar{\mathbf{B}} = \begin{bmatrix} \sqrt{\kappa} & 0 \\ 0 & K_b \end{bmatrix}.$$

We then solve (25), with

$$\mathbf{P}_S = E[\bar{\mathbf{x}}\bar{\mathbf{x}}^T] = \begin{bmatrix} \Sigma & M_b \\ M_b^T & N_b \end{bmatrix}. \quad (29)$$

The error covariance for the backward filter is then:

$$\sigma_b^2 = E[e_2 e_2^T] = \Sigma - M_b - M_b^T + N_b, \quad (30)$$

where $e_2 = \phi - \hat{\phi}_b$.

4.1.3. Smoother Error The forward and backward estimates are not independent in general and will have a cross-correlation term as follows [32]:

$$\sigma_{fb}^2 := E[e_1 e_2^T] = \Sigma - M_f^T - M_b + \alpha \Sigma \beta, \quad (31)$$

where $\alpha = M_f^T \Sigma^{-1}$ and $\beta = \Sigma^{-1} M_b$ [27].

The overall smoother error is [32]:

$$\sigma^2 = \frac{\sigma_f^2 \sigma_b^2 - (\sigma_{fb}^2)^2}{\sigma_f^2 + \sigma_b^2 - 2\sigma_{fb}^2}. \quad (32)$$

The term σ_{fb}^2 is zero, and so the forward and backward estimates are independent, in case of the optimal estimator, so that (32) reduces to (11).

4.2. Comparison of the Errors

The error-covariances of the robust smoother and the optimal smoother for the uncertain system may be computed using the above technique using Lyapunov equation, as a function of Δ . Here, we choose a certain value of μ and the other parameters as used in Ref. [9], viz. $|\alpha|^2 = 1 \times 10^6 \text{ s}^{-1}$, $\kappa = 1.9 \times 10^4 \text{ rad/s}$, $\lambda = 5.9 \times 10^4 \text{ rad/s}$, $r_m = 0.36$ and $r_p = 0.59$. Due to the implicit dependence of \bar{R}_{sq} and σ_f^2 , we compute the smoothed mean-square error in each case by running several iterations until σ_f^2 is obtained with an accuracy of 6 decimal places. Fig. 1 shows the comparison for $\mu = 0.8$, which corresponds to 80% uncertainty in λ . At $\Delta = 0$, where the nominal parameters for the

model exactly match those of the system, the optimal smoother performs better than the robust smoother. This is to be expected because the smoother has been optimised for those parameters. However, the robust smoother error is lower than that of the optimal smoother as Δ approaches 1. We define $\sigma_w^2(\mu)$ as the worst-case estimation error for each value of μ , i.e. $\sigma_w^2(\mu) = \sigma^2(\Delta = 1, \mu)$. So, if our system is not allowed to exceed an error threshold of say 0.0282 for this level of uncertainty in λ , our robust estimator guarantees that the error is below this threshold, whereas the optimal estimator breaches it in the worst case.

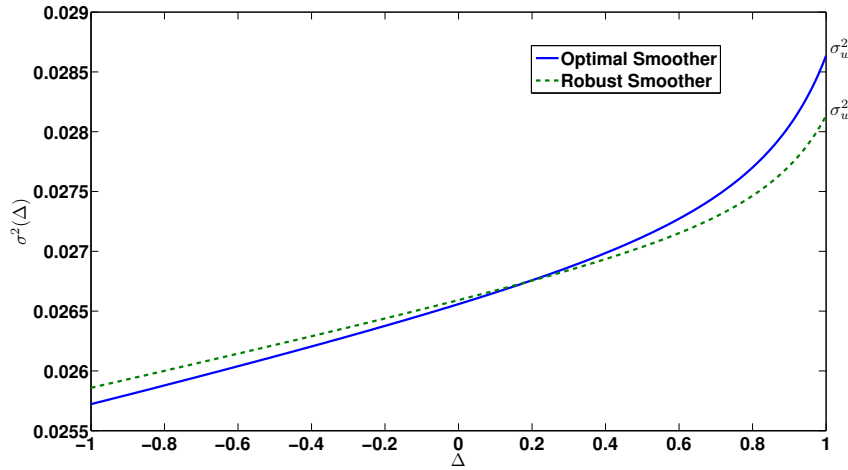


Figure 1. Ornstein-Uhlenbeck Noise: Comparison of estimators for extent of uncertainty $\mu = 0.8$. Here, $\sigma^2(\Delta)$ is the smoother error covariance of the optimal and robust estimators plotted as a function of the uncertain parameter $|\Delta| \leq 1$.

Fig. 2 shows the comparison of the worst-case performance of the optimal and the robust estimators for the uncertain system for $0 \leq \mu \leq 0.9$. Clearly, the robust estimator provides with better worst-case performance than the optimal estimator for all levels of uncertainty in λ . Also, the worst-case robust estimator error is below a desired threshold of say 0.029 for up to a higher level of uncertainty as compared to the optimal estimator. This is exactly the power of robust design techniques.

5. Resonant Noise Process

We now consider a second-order resonant noise process, typically produced by a piezo-electric transducer (PZT) driven by an input white noise. Such a resonant process is more complicated than the simplistic OU noise process considered before and better resembles the kind of noises that in practice corrupt the signal [38]. The simplified transfer function of a typical PZT is:

$$G(s) := \frac{\phi}{v} = \frac{\kappa}{s^2 + 2\zeta\omega_r s + \omega_r^2}, \quad (33)$$

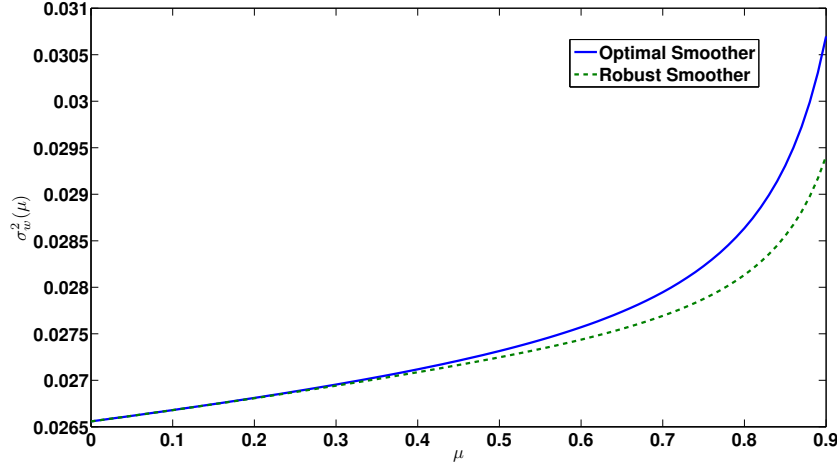


Figure 2. Ornstein-Uhlenbeck Noise: Comparison of worst-case error covariance as a function of μ . Here, $\sigma_w^2(\mu)$ is the worst-case smoother error covariance of the optimal and robust estimators plotted as a function of the extent of uncertainty $0 \leq \mu \leq 0.9$.

where κ is the gain, ζ is the damping factor, ω_r is the resonant frequency (rad/s), v is a zero-mean white Gaussian noise with unity amplitude and ϕ is the PZT output that modulates the phase to be estimated.

5.1. System Model (Exact)

A state-space realization of the transfer function (33) is:

$$\dot{\mathbf{x}} = \mathbf{A}\mathbf{x} + \mathbf{G}v, \quad (34)$$

where

$$\mathbf{x} := \begin{bmatrix} \phi \\ \dot{\phi} \end{bmatrix}, \quad \mathbf{A} := \begin{bmatrix} 0 & 1 \\ -\omega_r^2 & -2\zeta\omega_r \end{bmatrix}, \quad \mathbf{G} := \begin{bmatrix} 0 \\ \kappa \end{bmatrix}.$$

Eq. (34) constitutes our process model, whereas the measurement remains the same as (4). Thus, our measurement model is

$$\theta = \mathbf{H}\mathbf{x} + \mathbf{J}w, \quad (35)$$

where $\mathbf{H} := \begin{bmatrix} 2|\alpha|/\sqrt{R_{sq}} & 0 \end{bmatrix}$ and $\mathbf{J} := 1$.

5.2. Uncertain Model

We introduce uncertainty in \mathbf{A} as follows:

$$\mathbf{A} \rightarrow \mathbf{A} + \begin{bmatrix} 0 & 0 \\ -\mu\delta\omega_r^2 & 0 \end{bmatrix}, \quad (36)$$

where uncertainty is introduced in the resonant frequency ω_r through δ . Furthermore, $\Delta := \begin{bmatrix} \delta & 0 \end{bmatrix}$ is an uncertain parameter satisfying $\|\Delta\| \leq 1$ which implies $\delta^2 \leq 1$.

Moreover, $\mu \in [0, 1)$ determines the level of uncertainty. From Eq. (2.5) in Ref. [31], the uncertain process model here is:

$$\dot{\mathbf{x}} = (\mathbf{A} + \mathbf{G}\Delta\mathbf{K})\mathbf{x} + \mathbf{G}v, \quad (37)$$

where $\mathbf{K} := \begin{bmatrix} -\frac{\mu\omega_r^2}{\kappa} & 0 \\ 0 & 0 \end{bmatrix}$.

5.3. Comparison of the Estimators

The optimal and robust estimators can be constructed for the resonant noise case using the same method employed in the OU noise case before. The mean-square errors in estimation of ϕ may be computed using the error-analysis technique discussed before for both the optimal smoother and robust fixed-interval smoother as a function of the uncertain parameter δ . These values can be used to generate a plot of the errors versus δ for a given value of μ to compare the performance of the robust smoother and the optimal smoother for the uncertain system. It is also insightful to include in the graph the coherent state limit (CSL), which is the minimum theoretical error reachable with a coherent beam [9]. We as well include the standard quantum limit (SQL), which is the minimum phase estimation error that can be obtained with coherent beam using perfect heterodyne technique [32]. Fig. 3 shows the plot for $\mu = 0.8$. Here, we used a parameter regime particularly suited to the illustration of our key robustness results, viz. $\kappa = 9 \times 10^4$, $\zeta = 0.1$ and $\omega_r = 6.283 \times 10^3$ rad/s (1 kHz) and $\alpha = 5 \times 10^2$ s⁻¹. Also, we used $r_m = 0.48$ and $r_p = 1.11$ to have optimal squeezing level, for which the estimation error is the minimum for the exact model [9].

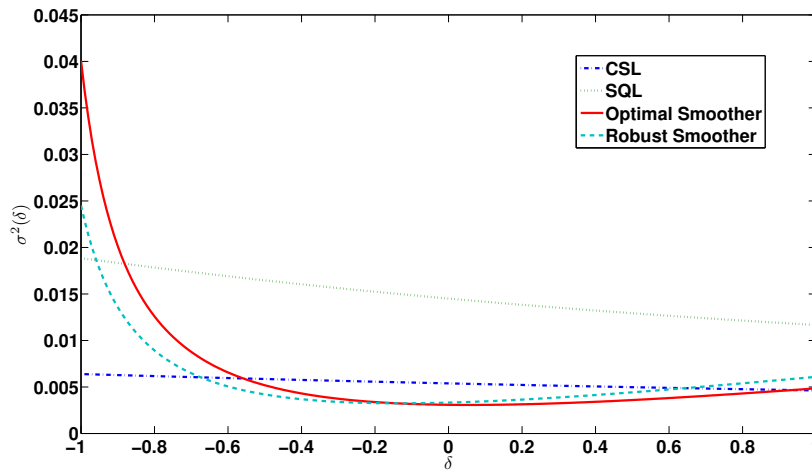


Figure 3. Resonant Noise: Comparison of the smoothers for uncertainty level $\mu = 0.8$. Here, $\sigma^2(\delta)$ is the smoother error covariance of the optimal and robust estimators plotted as a function of the uncertain parameter $|\delta| \leq 1$. Moreover, CSL = Coherent State Limit and SQL = Standard Quantum Limit.

One can see that the optimal smoother behaves better than the robust smoother

when $\delta = 0$, as expected. However, in the worst-case scenario, i.e. as δ approaches -1 , the performance of the robust smoother is superior to that of the optimal smoother. Nonetheless, we trade the best-case performance in achieving it. It is also of relevance that the robust estimator beats the SQL over a larger part of the uncertainty window than the optimal estimator, although so is not the case with respect to the CSL for this value of μ .

Fig. 4 depicts the worst-case performance of the estimators for $0 \leq \mu \leq 0.9$. Clearly, the robust estimator outperforms the optimal estimator in the worst-case for all levels of μ . Also shown in the plot are the SQL and the CSL. If the SQL or the CSL is considered as the allowed threshold for the estimation error, our robust estimator provides guaranteed worst-case performance below this threshold for up to a larger uncertainty level when compared to the optimal estimator.

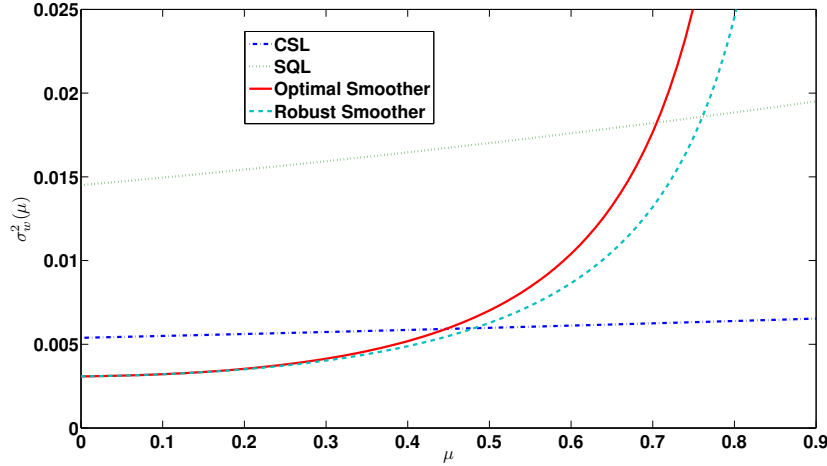


Figure 4. Resonant Noise: Comparison of worst-case error covariance as a function of μ . Here, $\sigma_w^2(\mu)$ is the worst-case smoother error covariance of the optimal and robust estimators plotted as a function of the extent of uncertainty $0 \leq \mu \leq 0.9$. Moreover, CSL = Coherent State Limit and SQL = Standard Quantum Limit.

Moreover, the improvement with the robust smoother over the optimal smoother is better with the resonant noise process considered here as compared to that with OU noise process considered before. For example, while the worst-case improvement for 80% uncertainty in the OU noise case was ~ 0.08 dB, that in this resonant noise case is ~ 2.13 dB. Indeed, OU noise is the output of a non-resonant low-pass filter (LPF), driven by white noise. Any uncertainty in the corner frequency of the LPF, represented by λ here, would not change the magnitude of the phase noise as much as an equivalent amount of uncertainty in the resonant frequency ω_r for the resonant noise model. In fact, the relative performance of our robust estimator grows as the noise process becomes more resonant. This is shown in Fig. 5, which plots the worst-case errors of the optimal and robust smoothers as a function of the damping factor ζ , that determines the degree of resonance; i.e. lower the damping factor, more resonant the process is. Here, at each

value of ζ , the squeezing level has been optimized to yield the minimum error for the exact model.

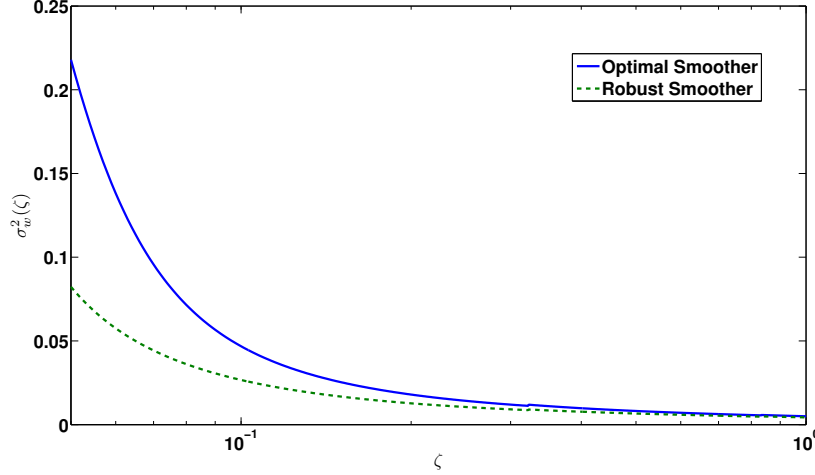


Figure 5. Resonant Noise: Comparison of worst-case error covariance as a function of ζ . Here, $\sigma_w^2(\zeta)$ is the worst-case smoother error covariance of the optimal and robust estimators plotted as a function of the damping factor ζ varying from 0.05 to 1.

Fig. 6 shows a plot of the worst-case errors of the smoothers as functions of the squeezing level. Here, we have plotted the errors for pure lossless squeezed beams (overall loss $l_{sq} = 0$) and practical impure lossy squeezed beams with $l_{sq} = 0.33$ (See supplementary material for Ref. [9]), and a fixed uncertainty level of $\mu = 0.4$. Clearly, our robust estimator not only beats the CSL over a wider range of squeezing levels (for both pure and impure squeezing cases), but also can sustain higher levels of squeezing than the optimal estimator can, before the errors rapidly increase due to excessive anti-squeezing noise. Moreover, our estimator is more robust relative to the optimal estimator for practical squeezed beams than for ideal pure squeezed beams. This is due to the larger worst-case performance benefit obtained in the practical case than in the ideal case at the optimal squeezing levels. That is, our estimator, that was designed to be robust to uncertainty in the resonant frequency ω_r , is also robust, relative to the optimal estimator, against the overall loss l_{sq} , arising from imperfect detectors, the OPO and modulators.

Finally, we plot the worst-case errors of the estimators against the photon number in Fig. 7. Here, at each value of α , the squeezing level has been optimized to yield the least worst-case robust estimation error. One can choose to optimize the squeezing level on a different basis as well. Interestingly, not only the two errors scale differently with the photon number, we also note that there exists an optimum photon number, for which the robust estimator provides the best worst-case performance compared to the optimal estimator. This is quite significant, given how important the achievable precision for available finite quantum resources in practice is.

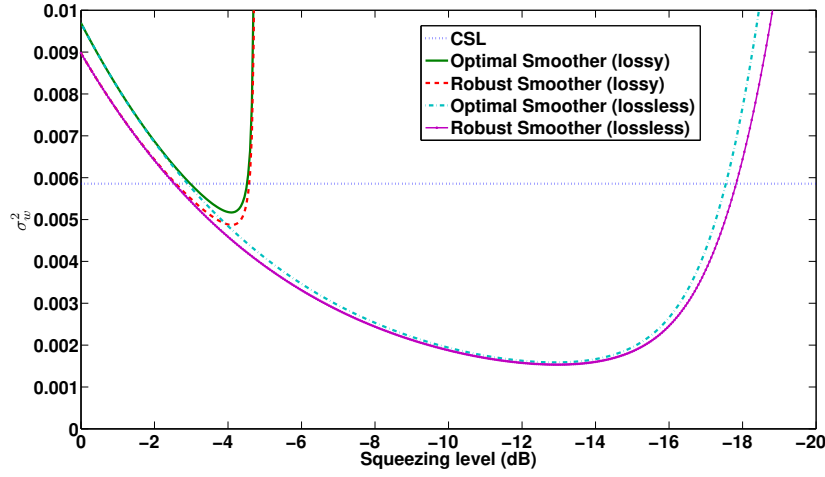


Figure 6. Resonant Noise: Comparison of worst-case error covariance as a function of squeezing level. Here, σ_w^2 is the worst-case smoother error covariance of the optimal and robust estimators plotted as a function of the squeezing level varying from 0 to -20 dB. Moreover, CSL = Coherent State Limit.

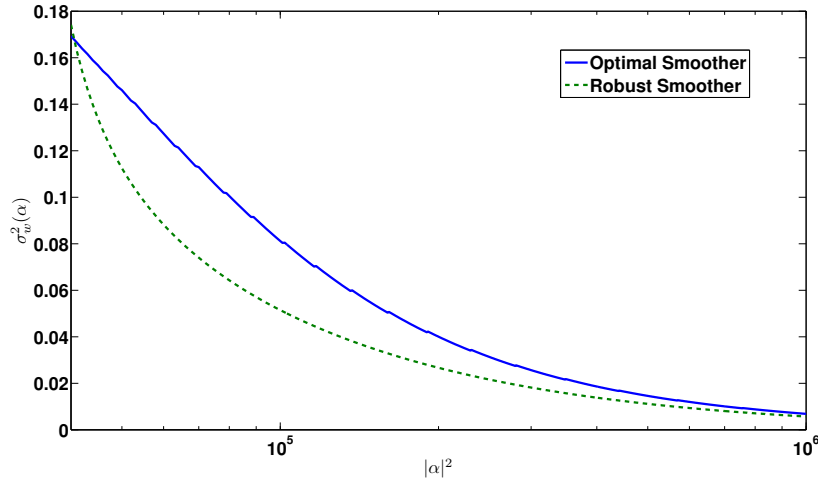


Figure 7. Resonant Noise: Comparison of worst-case error covariance as a function of photon number. Here, $\sigma_w^2(\alpha)$ is the worst-case smoother error covariance of the optimal and robust estimators plotted as a function of the photon number varying from 4×10^4 to 10^6 s^{-1} .

6. Conclusion

This work considered robust quantum phase estimation with explicitly modelled uncertainty introduced in the underlying system in a systematic state-space setting within the modern control theory paradigm. In particular, we constructed a robust fixed-interval smoother for continuous phase estimation of a squeezed state of light with uncertainty considered in the phase noise. We illustrated that our robust estimator provides guaranteed worst-case performance as desired. We showed that the worst-case

performance of our robust estimator with respect to the optimal estimator improves with more resonance in the phase noise. Moreover, we found that robustness is more useful for practical lossy squeezed beams, when compared to pure squeezed beams, ideally limited by Heisenberg's uncertainty principle. In addition, we saw that there is an optimal photon number for which the performance of the robust estimator relative to the optimal estimator is the best. These results demonstrate the significant impact that the rich theory of classical robust estimation can have on improving quantum parameter estimation. They can pave the way for tackling practical challenges owing to unavoidable parametric uncertainties facing quantum parameter estimation.

Acknowledgments

This work was supported by the Australian Research Council. The first author would like to thank Dr. Hongbin Song, Dr. Obaid Ur Rehman, Trevor Wheatley, Prof. Howard Wiseman and Dr. Dominic Berry for useful discussion and feedback related to this work.

References

- [1] Wiseman H M and Milburn G J 2010 *Quantum Measurement and Control* (Cambridge University Press)
- [2] Hofheinz M, Wang H, Ansmann M, Bialczak R C, Lucero E, Neeley M, O'Connell A D, Sank D, Wenner J, Martinis J M and Cleland A N 2009 *Nature (London)* **459** 546–549
- [3] Slavik R, Parmigiani F, Kakande J, Lundstrom C, Sjodin M, Andrekson P A, Weerasuriya R, Sygletos S, Ellis A D, Gruner-Nielsen L, Jakobsen D, Herstrom S, Phelan R, O'Gorman J, Bogris A, Syvridis D, Dasgupta S, Petropoulos P and Richardson D J 2010 *Nature Photonics* **4** 690–695
- [4] Chen J, Habif J L, Dutton Z, Lazarus R and Guha S 2012 *Nature Photonics* **6** 374
- [5] Inoue K, Waks E and Yamamoto Y 2002 *Physical Review Letters* **89** 037902
- [6] Giovannetti V, Lloyd S and Maccone L 2011 *Nature Photonics* **5** 222
- [7] Goda K, Miyakawa O, Mikhailov E E, Saraf S, Adhikari R, McKenzie K, Ward R, Vass S, Weinstein A J and Mavalvala N 2008 *Nature Physics* **4** 472–476
- [8] Wheatley T A, Berry D W, Yonezawa H, Nakane D, Arao H, Pope D T, Ralph T C, Wiseman H M, Furusawa A and Huntington E H 2010 *Physical Review Letters* **104** 093601
- [9] Yonezawa H, Nakane D, Wheatley T A, Iwasawa K, Takeda S, Arao H, Ohki K, Tsumura K, Berry D W, Ralph T C, Wiseman H M, Huntington E H and Furusawa A 2012 *Science* **337** 1514
- [10] Lewis F L, Xie L and Popa D 2008 *Optimal and Robust Estimation - With an Introduction to Stochastic Control Theory* 2nd ed (CRC Press, Taylor & Francis Group)
- [11] Zhou K, Doyle J C and Glover K 1996 *Robust and Optimal Control* (Prentice-Hall)
- [12] Stockton J K, Geremia J M, Doherty A C and Mabuchi H 2004 *Physical Review A* **69** 032109
- [13] Yamamoto N 2006 *Physical Review A* **74** 03217
- [14] James M R, Nurdin H I and Petersen I R 2008 *IEEE Trans. on Automatic Control* **53** 1787
- [15] Wiseman H M 1995 *Physical Review Letters* **75** 4587–4590
- [16] Wiseman H M and Killip R B 1997 *Physical Review A* **56** 944–957
- [17] Wiseman H M and Killip R B 1998 *Physical Review A* **57** 2169–2185
- [18] Pope D T, Wiseman H M and Langford N K 2004 *Physical Review A* **70** 043812
- [19] Armen M A, Au J K, Stockton J K, Doherty A C and Mabuchi H 2002 *Physical Review Letters* **89** 133602
- [20] Berry D W and Wiseman H M 2000 *Physical Review A* **63** 013813

- [21] Berry D W and Wiseman H M 2002 *Physical Review A* **65** 043803
- [22] Tsang M, Shapiro J H and Lloyd S 2009 *Physical Review A* **79** 053843
- [23] Tsang M 2009 *Physical Review Letters* **102** 250403
- [24] Ljung L and Kailath T 1976 *Automatica* **12** 147–157
- [25] Meditch J S 1973 *Automatica* **9** 151–162
- [26] Fraser D C and Potter J E 1969 *IEEE Transactions on Automatic Control* **14** 387–390
- [27] Wall Jr J E, Willsky A S and Sandell Jr N R 1981 *Stochastics* **5** 1–41
- [28] Mayne D Q 1966 *Automatica* **4** 73–92
- [29] Fraser D C 1967 *A New Technique for the Optimal Smoothing of Data* Sc.d. dissertation Massachusetts Institute of Technology, Cambridge, MA
- [30] Mehra R K 1967 *Studies in Smoothing and in Conjugate Gradient Methods Applied to Optimal Control Problems* Ph.d. dissertation Harvard University, Cambridge, MA
- [31] Moheimani S O R, Savkin A V and Petersen I R 1998 *IEEE Trans. on Circuits and Systems I - Fundamental Theory and Appl.* **45** 446
- [32] Roy S, Petersen I R and Huntington E H 2013 Adaptive continuous homodyne phase estimation using robust fixed-interval smoothing *Proceedings of the American Control Conference* pp 3129–3134
- [33] Roy S, Petersen I R and Huntington E H 2013 Robust phase estimation of squeezed state *Proceedings of the Conference on Lasers and Electro-Optics* p JTh2A.88
- [34] Roy S, Rehman O, Petersen I R and Huntington E H 2014 Robust smoothing for estimating optical phase varying as a continuous resonant process *Proceedings of the European Control Conference* pp 896–901
- [35] Roy S, Petersen I R and Huntington E H 2012 Robust filtering for adaptive homodyne estimation of continuously varying optical phase *Proceedings of the Australian Control Conference* pp 454–458
- [36] Roy S, Petersen I R and Huntington E H 2013 Robust estimation of optical phase varying as a continuous resonant process *Proceedings of the Multiconference on Systems and Control* pp 551–555
- [37] Brown R G 1983 *Introduction to Random Signal Analysis and Kalman Filtering* (John Wiley & Sons)
- [38] Iwasawa K, Makino K, Yonezawa H, Tsang M, Davidovic A, Huntington E and Furusawa A 2013 *Physical Review Letters* **111** 163602